



HAL
open science

A macro-array-based screening approach to identify transcriptional factors involved in the nitrogen-related root plasticity response of *Arabidopsis thaliana*

Timothy Tranbarger, Yves Al-Ghazi, Bertrand Muller, Bernard Teyssendier de La Serve, Patrick Doumas, Bruno Touraine

► To cite this version:

Timothy Tranbarger, Yves Al-Ghazi, Bertrand Muller, Bernard Teyssendier de La Serve, Patrick Doumas, et al.. A macro-array-based screening approach to identify transcriptional factors involved in the nitrogen-related root plasticity response of *Arabidopsis thaliana*. *Agronomie*, 2003, 23 (5-6), pp.519-528. 10.1051/agro:2003024 . hal-00886205

HAL Id: hal-00886205

<https://hal.science/hal-00886205>

Submitted on 11 May 2020

HAL is a multi-disciplinary open access archive for the deposit and dissemination of scientific research documents, whether they are published or not. The documents may come from teaching and research institutions in France or abroad, or from public or private research centers.

L'archive ouverte pluridisciplinaire **HAL**, est destinée au dépôt et à la diffusion de documents scientifiques de niveau recherche, publiés ou non, émanant des établissements d'enseignement et de recherche français ou étrangers, des laboratoires publics ou privés.

A macro-array-based screening approach to identify transcriptional factors involved in the nitrogen-related root plasticity response of *Arabidopsis thaliana*

Timothy J. TRANBARGER^{a,c}, Yves AL-GHAZI^a, Bertrand MULLER^b, Bernard TEYSSENDIER DE LA SERVE^a, Patrick DOUMAS^a, Bruno TOURAINE^{a,c*}

^a Laboratoire de Biochimie et Physiologie Moléculaire des Plantes, UM2/INRA/Agro-M/CNRS UMR 5004, place Viala, 34060 Montpellier Cedex 1, France

^b Laboratoire d'Écophysiologie des Plantes sous Stress Environnementaux, INRA/Agro-M, place Viala, 34060 Montpellier Cedex 1, France

^c Present address: Laboratoire des Symbioses Tropicales et Méditerranéennes, UM2/CIRAD/IRD/INRA/Agro-M UMR 1063, Université Montpellier II, C.C. 002, place Eugène Bataillon, 34095 Montpellier Cedex 05, France

(Received 25 July 2002; accepted 29 April 2003)

Abstract – We examined changes in the root architecture and morphology of *Arabidopsis thaliana* grown on vertically-oriented agar plates containing 0.1, 0.5 or 10 mM KNO₃, or 0.5 mM KNO₃ supplemented with 5 mM glutamine or asparagine. The roots of 14-day-old plants grown with 10 mM KNO₃ had the least number and length of lateral roots (LR) in contrast to plants grown on the other nitrogen sources. NO₃⁻ inhibited LR development at a stage after the initiation of primordia and before emergence of the LR. To identify the regulatory genes involved in the root response, we constructed a macro-array that contained 126 putative transcriptional factor ESTs to analyze their expression profiles. Expression patterns in roots or shoots of plants grown on different N sources indicated that only a limited number of genes responded. The highest level of variation in expression was obtained when comparing the roots of plants supplied with 10 mM versus 0.5 mM NO₃⁻.

gene expression / lateral root / macro-array / nitrogen / root architecture / transcription factor

Résumé – Utilisation de macro-arrays pour identifier des facteurs de transcription impliqués dans la réponse de plasticité racinaire à l'azote chez *Arabidopsis thaliana*. Des plantes d'*Arabidopsis thaliana* sont cultivées dans des boîtes de Pétri verticales, sur un milieu gélosé où l'azote est apporté sous forme de KNO₃ 0,1, 0,5 ou 10 mM, ou de KNO₃ 0,5 mM additionné de glutamine ou d'asparagine 5 mM. Le traitement KNO₃ 10 mM correspond aux plus faibles nombre et longueur de racines latérales. Leur développement est inhibé à un stade postérieur à l'initiation des primordia et antérieur à leur émergence. Des membranes Nylon (macro-arrays) contenant 126 EST de facteurs de transcription potentiels sont construites afin d'identifier des gènes régulateurs impliqués dans cette réponse d'architecture racinaire. L'analyse des profils d'expression dans les racines et les parties aériennes de plantes cultivées sur les différentes sources d'azote indiquent que les gènes répondant aux traitements sont peu nombreux, et que la plus forte variation est obtenue lorsque l'on compare les traitements KNO₃ 10 mM et KNO₃ 0,5 mM.

expression génétique / racine latérale / macro-array / azote / architecture racinaire / facteur de transcription

1. INTRODUCTION

The growth and development of a plant depends on the capacity of the root system to explore the soil and to respond to localized changes in nutrient availability. Except for C, H and O, all the elements essential to the plant are foraged by roots as mineral ions from the soil. The architecture of the plant root system has the capacity to respond accordingly to changes in mineral ion availability. This root plasticity in

response to changes in mineral ion availability has been shown experimentally by either providing localized sources of specific nutrients [1, 5, 14] or by changing the overall availability of a given nutrient to the whole root system [7]. Considering the quantitative importance of nitrogen for plant growth compared with other elements taken up from the soil, root plasticity is especially important in terms of N nutrition and the ability of roots to take up sufficient amounts of NO₃⁻, the preferred N source for most plants. Plants supplied with low

Communicated by Philippe Hinsinger (Montpellier, France)

* Correspondence and reprints
touraine@univ-montp2.fr

amounts of NO_3^- typically have a lower shoot:root ratio than adequately-supplied plants [3, 9, 15]. This shift in biomass allocation tends to reduce the demand factor for NO_3^- when this ion is present in very low concentrations at the root:soil interface, and usually involves a concomitant decrease in the shoot growth rate and increase in the root growth rate. Globally, these developmental changes are similar to those observed when H_2PO_4^- or SO_4^{2-} supply is limited, which suggests a general adjustment to low nutrient availability rather than a specific response to NO_3^- or a NO_3^- -derived signal [4]. However, changing the availability of NH_4^+ does not trigger similar root responses [19], indicating some specificity of the mechanisms involved.

Tobacco transformants with low nitrate reductase activity exhibit a higher accumulation of NO_3^- and a higher shoot:root ratio than N-replete wild-type plants [15], despite the fact the low-nitrate reductase plants were severely N-limited with respect to organic nitrogen. This suggests NO_3^- ions themselves are involved in the phenotypic adjustments to changes in external NO_3^- concentration, rather than a metabolite downstream of N assimilation. More specifically, root growth inhibition was triggered by NO_3^- accumulation in the shoot but not in the root, as shown in split-root experiments [15], indicative of a systemic regulation that involves interorgan signaling. However, it is well documented that NO_3^- is quasi-excluded from the sieve sap; therefore, an unidentified NO_3^- -related signal must be translocated from the shoots to the roots. The inhibition of root biomass accumulation by high tissue NO_3^- corresponded to a decrease in the number of lateral roots for both wild-type and low-nitrate reductase transformants of tobacco, while the growth rate of the primary root was not affected [15, 16].

The root developmental response to changes in NO_3^- availability is complex. An increase in NO_3^- levels can also have a positive effect on root development. Locally applied NO_3^- leads to a concomitant stimulation of lateral root proliferation in the same area [6, 8, 13], a response independent of metabolites downstream of the NO_3^- assimilation in tobacco [15] and *Arabidopsis thaliana* [20]. In addition, this response is not associated with an increase in local concentrations of amino acids or protein [15], consistent with the hypothesis that it is a NO_3^- -mediated signaling rather than a simple nutrient-mediated stimulation of root growth. The NO_3^- -inducible root-specific gene *ANR1*, which encodes a MADS box transcription factor, has been identified as a component of the signaling pathway involved in the stimulation of lateral root growth in response to a localized supply of NO_3^- in *A. thaliana* [20]. The use of *ANR1*-repressed lines (antisense or co-suppressed sense) demonstrated a role for *ANR1* in eliciting the developmental response to localized NO_3^- supply. The enhanced development of lateral roots was due to a marked increase in their elongation rate and attributed to an increase in the rate of cell production in their meristem [20]. In addition, the *A. thaliana* auxin-resistant mutant *axr4* did not exhibit lateral root proliferation in response to localized NO_3^- treatment, which suggests an overlap between the NO_3^- and the auxin response pathways [20].

In addition to the stimulatory effect localized NO_3^- has on lateral root development, high NO_3^- can also inhibit lateral root growth when supplied evenly to the entire root system.

Furthermore, lateral root development in the *ANR1* antisense lines was more sensitive to high NO_3^- concentrations (i.e. more inhibited) and the sensitivity increased with the degree of *ANR1* repression in the transgenic lines [20]. These observations are consistent with the hypothesis that NO_3^- regulates root branching via dual mechanisms: the inhibitory effect of NO_3^- is more pronounced in the *ANR1*-deficient plants due to the lack of the *ANR1*-dependent localized stimulatory effect. The dual-pathway model comprises a localized stimulation of lateral root development by NO_3^- and a systemic inhibition of lateral root development by high tissue NO_3^- [20, 21]. While *ANR1* and *AXR4* have been shown to be involved in the localized NO_3^- stimulation pathway, no component of the systemic pathway has been identified. The objectives of the present study are to examine the root architecture and morphology of *A. thaliana* in response to various N treatments in order to select the appropriate culture conditions to screen for regulatory genes involved in the systemic NO_3^- regulation pathway, using a transcription factor macro-array. The results of the architecture/morphology analysis and the global results from the macro-array hybridizations from selected culture conditions are presented.

2. MATERIALS AND METHODS

2.1. Plant growth and treatments applied

Seeds of *Arabidopsis thaliana* ecotype Columbia were surface-sterilized in 2% Bayrochlor (Baylor) and 50% ethanol with agitation for 20 min followed by 3 rinses with 100% ethanol and three rinses with sterile distilled H_2O . Seeds were pipetted onto 12-cm-square Petri plates (5 seeds per plate, at ca. 2 cm from the top) containing the following medium: 0.8% agar, 0.5 mM KNO_3 , 0.5 mM CaSO_4 , 1 mM KH_2PO_4 , 0.5 mM MgCl_2 , 0.05 mM NaFeEDTA , 12 μM H_3BO_3 , 1 μM MnCl_2 , 1 μM $\text{H}_2\text{4MO}_7\text{N}_6\text{O}_{24}$, 0.03 μM ZnCl_2 and 2.5 mM MES (2-[Morpholino]ethanesulfonic acid, Sigma), pH 5.7. The agar media were segmented into 2 layers by a 0.5-cm-wide gap at approximately 3 cm from the top of the plates, and the bottom layer was supplemented with either 9.5 mM KNO_3 or 5 mM amino acid, depending on the treatment. The gap that separated these two parts prevented any significant diffusion of N nutrients from one layer to the other (checked by chemical assays of NO_3^- and amino acids). The reason for segmenting the agar plates was it allowed the initial (germination) phase to occur under standard and identical conditions in all treatments. The primary root entered the lower part, where the treatments were applied, on day 5. Plates with seeds were stored at 4 °C for 24–48 h before being placed vertically into a controlled environmental room at 20 °C constant day and night temperature with a photoperiod of 16 h light (150 $\mu\text{mol}\cdot\text{m}^{-2}\cdot\text{s}^{-1}$). This light condition allowed root elongation and branching to proceed without the need for a C source (such as sucrose) in the root medium.

2.2. Root architecture analysis

Petri plates were scanned to a resolution of 400 dpi at day 14, just before the primary root reached the bottom of the

plate. Scanned images were saved as TIF files and the root architecture was analyzed using Optimas image analysis software (Media Cybernetics, Silver Spring, MD – USA). The images were analyzed to measure the length of the primary root, the length of each lateral root and the distance from the primary root base to the insertion point of each lateral root. For standardization, we decided not to take into account lateral roots whose length was less than a threshold value set at twice the primary root diameter, i.e. 0.25–0.30 mm. Root and shoot tissues were collected at day 14 for cDNA synthesis and macro-array hybridizations (see below).

2.3. Macro-array preparation

A. thaliana expressed sequence tags (ESTs) with similarity to transcription factors were selected by BLAST searching an EST database provided by Drs. Hoheisel and Scheideler (Deutsches Krebsforschungszentrum, Heidelberg, Germany). The transcription factor clones selected represent the ESTs available at the time the macro-array was constructed. Several other cDNA and control clones were also selected based on their proposed role in root development and/or nitrogen nutrition. The entire list of clones spotted on the membrane are given in Table 1. Inserts were amplified by polymerase chain reaction (PCR) in 50 μ L reaction volumes with M13 Forward and Reverse primers. After each PCR reaction, 2 μ L was electrophoresed on agarose gels to assess the quantity and quality of the amplified product. Approximately 15 reactions per clone were performed and the products were pooled and precipitated at -20°C with 1:10 volume 3 M sodium acetate (pH 5.2) and 2.5 volumes ethanol. Precipitated PCR products were centrifuged at 7000 g for 30 min, 4°C , and the pellets were rinsed with 70% ethanol, centrifuged at 10000 g for 10 min, 4°C , and stored at -20°C . Prior to spotting, pellets were resuspended in 40 μ L sterile H_2O and 2 μ L was electrophoresed on agarose gels to assess the quantity and quality of the final product. PCR products were denatured at 95°C and arrayed by robotics onto Nylon membranes (Biotrans, ICN). Macro-arrays were prepared and processed according to Bertucci et al. [2].

2.4. Total RNA extraction, cDNA synthesis and labeling

For macro-array hybridizations, total RNA was isolated from 14-day-old plants grown with the N sources and under the conditions described above. Roots and shoots were separated, frozen in liquid nitrogen and stored at -80°C until RNA was extracted. Total RNA was extracted from tissues using TRizol reagent (Life Technologies, Invitrogen, Carlsbad CA) according to the manufacturer.

For each cDNA synthesis labeling reaction, oligo dT primers (0.5 μ L 20 μM oligo-dT₁₂₋₁₈ + 0.5 μ L 20 μM oligo-dT₂₅₋₃₀) were added to 25 μg (9 μ L) of total RNA and incubated for 10 min at 70°C . Primers were annealed by allowing them to cool slowly to 43°C and subsequently 6 μ L RT buffer, 3 μ L 0.1 M DTT, 3 μ L 10 mM dAGT-mix, 3 μ L 50 μM unlabeled dCTP, 3 μ L 10 μCi μL^{-1} [^{33}P] dCTP and 2 μ L 200 U μL^{-1} Superscript RT II (Life Technologies) were added for a final volume of 30 μ L. The reverse transcription reaction mix was incubated at 42°C for 1 hour and subsequently RNA was

hydrolyzed by the addition of 1 μ L 1% SDS, 1 μ L 0.5 M EDTA and 3 μ L 3 M NaOH with incubation at 65°C for 30 min followed by 15 min at room temperature. The mixture was neutralized with the addition of 10 μ L 1 M Tris-HCL (pH 8.3) and 3 μ L 2 N HCl, and the cDNA was precipitated with the addition of 5 μ L 3 M sodium acetate (pH 5.3), 5 μ L 10 $\text{mg}\cdot\text{mL}^{-1}$ tRNA and 60 μ L isopropanol, and incubated at -20°C for 30 min. The precipitated cDNA was centrifuged at 16000 g for 30 min at room temperature, the supernatant was removed, and the pellet was resuspended in 100 μ L of H_2O .

2.5. Macro-array hybridization and image analysis

Two sets of macro-array hybridizations were performed on two replicate biological experiments and 3 membranes were used for each hybridization. Macro-arrays were prehybridized for 30 min at 65°C in Church buffer (0.5 mM sodium phosphate pH 7.2, 7% [w/w] SDS and 1 mM EDTA) containing 100 $\mu\text{g}\cdot\mu\text{L}^{-1}$ tRNA. The labeled cDNA was denatured at 95°C for 5 min and added to the prehybridization solution and hybridized for 14 h at 65°C in a hybridization oven. The hybridization solution was poured off, rinsed quickly with washing buffer (40 mM sodium phosphate pH7.2 and 0.1% [w/w] SDS), and the membrane was washed for 20 min at 65°C in washing buffer. Membranes were wrapped in plastic and exposed to a phosphor screen for typically 3–5 days. Screens were scanned at a resolution of 50 microns with a phospho-imager (Storm, Molecular Dynamics), images were saved as TIF files and spot intensities were quantified with SCANALYZE (Michael Eisen, Lawrence Berkeley National Lab.). An average background value from 40 empty spots was subtracted from each spot intensity, which was then normalized by dividing by the average intensity value of the sum of all the spot intensities.

3. RESULTS

The control treatment was defined as 0.5 mM NO_3^- because at that concentration, growth for 14 days on vertical Petri plates is optimum, the high-affinity NO_3^- transport systems operate at maximum velocity, and only a minimum of N depletion occurs from the agar (data not shown). Plants were scanned after 14 days of growth and representative images are shown in Figure 1. A low (0.1 mM) NO_3^- concentration reduced primary root length and increased secondary root length (Fig. 1). A high NO_3^- concentration (10 mM) had little impact on primary root length but dramatically reduced lateral root development. Little additional effect was found when plants were grown on 20 mM NO_3^- (data not shown). Adding 9.5 mM KCl instead of 9.5 mM KNO_3 led to no change in root architecture (data not shown), indicating that the changes were the result of the increase in NO_3^- , not K^+ concentration. Supplying organic nitrogen (Gln and Asn) at high concentration (10 mM N) had an opposite impact as compared with the high NO_3^- treatment: visually, both Gln and Asn appeared to increase the number and length of lateral roots (Fig. 1). In the case of Asn, however, the effect on lateral root development seemed to be accompanied by a significant decrease in primary root length.

Table I. EST clones with sequence similarities to transcription factors, in addition to control clones and other known cDNAs spotted on the membrane. Similarities to transcription factors are based on BLAST searches using each of the partial EST sequences that correspond to the clone ID number. Where the gene names are listed, full-length cDNA clones were spotted on the membrane.

	Clone Id or gene name	Nearest BLAST sequence similarity
Zinc Finger Factor Families	162M1T7	ZAT10 zinc finger protein
	65F10T7	ZAT12 zinc finger protein
	103p14t7	c2h2 zinc finger protein
	245B19T7	AZF3 c2h2 zinc fing prot-3
	209B3T7	CCCH-type zinc finger protein
	230J15T7	CCCH-type zinc finger protein
Cat-Box Binding Proteins	77G8T7	Hap3a CCAAT box binding protein
	198M21T7	Hap3b CCAAT box binding protein
	247D4T7	Hap3b CCAAT box binding protein
	119P10T7	Hap5a CCAAT box binding protein
	123H3T7	Hap5b CCAAT box binding protein
CCR4-Associated-Like Factors	73d4t7	putative CCR4 associated factor
	195M6T7	putative CCR4 associated factor
	201N17T7	putative CCR4 associated factor
	VBVCA03	putative CCR4 associated factor
TFIID Related Factors (TATA Binding Factors)	G1C10T7	TFIID-1
	114F16T7	TATA sequence-binding protein I
	92N6T7	transcription initiation factor II
	103d19t7	Factor required for mammalian TFIID
G-Box Binding Factors (bZIP)	108h2t7	TGA1/Gbox binding factor/leucine zipper
	149J19T7	TGA3-like bZIP
	181F23T7	TGA family of bZIP
	191D1T7	TGA1, TF:basic leucine zipper domain
	251P4T7	Similar to TAG1 bZIP
	121F19T7	Similar to TAG1 bZIP
	135H14T7	G-box binding factor
	157H19T7	Leu/Zip binds G-box-like
	185A23T7	GBF1, G-box binding factor 1
	195C13T7	G-box binding protein
	VBVJH12	GBF3,G-box factor 3
	VBOB03	GBF3, G-box factor 3
	Other bZIP-Like Factors	181C12T7
183B23T7		bZIP-like DNA-binding protein
211F11T7		bZIP-like DNA binding protein
E2G8T7		bZIP-like DNA binding protein
E12D2T7		CPRF2, DNA-binding protein
128G24T7		bZIP-like DNA binding protein
Scarecrow-Like Factors (SCR bZIP-like domain)	VBVIH03	SCL1, scarecrow-like 1
	200M14T7	SCL8, scarecrow like 8
	147F19T7	SCL9, scarecrow like 9
	153I23T7	SCL11,scarecrow like 11
	211P20T7	SCL13, scarecrow like 13
Myb-Like Factor Family	122N17T7	MYB6, DNA-binding protein
	194F2T7	MYB12, R2R3-MYB family member
	170K1T7	MYB45, R2R3-MYB family member
	99M15T7	MYB51, R2R3-MYB family member
	114F24T7	MYB59, R2R3-MYB, family member
	206N11T7	MYB59, R2R3-MYB family member
	106h10t7	MYB63, R2R3-MYB family member
	110f12t7	MYB68, R2R3-MYB family member
	193M15T7	MYB90, R2R3-MYB family member

Table I. Continued.

	157G9T7	MYB92, R2R3-MYB family member
	178M4T7	MYB93, R2R3-MYB family member
	162I3T7	MYB (late elongated hypocotyl)
	VBVXF11	MYB (late elongated hypocotyl)
	186O19T7	MYB homologue (mixta gene)
	VBVCE07	HSR1 Myb-like protein
	109K9T7	MYB-related protein
	137A5T7	MYB-related protein
	198N20T7	R2R3-MYB factor
	226M4T7	Myb-related (MybSt1 isolog)
	H9E8T7	MYB family member
	VBVVE03	MYB family member
MADS-Box AP1-Like Factors	113f9t7	AP1, homeotic/flower/MADS box
	182B3T7	AGL9, MADS box protein
	201N18T7	AGL11, MADS box protein
	171E11T7	AGL15, MADS box protein
	181D16T7	AGL17, MADS box protein
	Anr1	ATANR1 MADS box protein
AP2 Domain Containing Factors	131F22T7	RAP2.2, AP2 domain protein
	120H10T7	RAP2.2, AP2 domain protein
	227C4T7	RAP2.4, AP2 domain protein
	142G24T7	RAP2.5, AP2 domain protein
	227N9T7	RAP2.5, AP2 domain protein
	132C14T7	RAP2.6, AP2 domain protein
	155P21T7	CKCW/2 AP2 domain protein
	139E24T7	pFAM domain/AP2 domain protein
	185C24T7	putative AP2 domain protein
Homeodomain Proteins	151M10T7	homeodomain protein AHDP, ATML1-like
	214H17T7	ATML1, homeodomain protein
	F1A7T7	ANL2, homeodomain protein
	224P9T7	ANL2, homeodomain protein
	VBVNG06	Anthocyaninless2-(ANL2)-like
Auxin Response Factors	161D7T7	ARF6, binds ARE
	G2H12T7	ARF1, binds ARE
	244A1T7	ARF1, binds ARE
	115E7T7	ARF4, binds ARE
	VBVWA07	ARF8, binds ARE
	170G16T7	IAA response nuclear protein
	E7A12T7	IAA2, auxin-response nuclear protein
	E8D3T7	IAA3, auxin-response nuclear protein
	G5C3T7	IAA4, auxin-response nuclear protein
	196F10T7	IAA9, auxin-response nuclear protein
	210I12T7	IAA9-like
	air1	auxin-induced lateral root/C-terminus of putative plasma membrane-cell wall linker*
	lrp1	auxin-induced lateral root primordia (LRP1)
L2/LIM-Like Factors	111C13T7	ATL1, LIM 1 protein
	117H2T7	ATL2, LIM domain protein PLIM-2
	E3E11T7	ATL2, LIM domain protein PLIM-2
	E8G5T7	ATL2, LIM domain protein PLIM-2
	193P8T7	ATL2, LIM domain protein PLIM-2
GATA-Binding Factors	VBVXC08	AtGATA 2, GATA-binding protein
	164D22T7	GATA 3, GATA-binding protein
	E1C2T7	GATA4, GATA-binding protein

Table I. Continued.

Heatshock Transcription Factors	169E3T7	HSF30 homolog
	200M20T7	HSF30 homolog
	167D24T7	HSF-type DNA-bind domain
	172M1T7	HS factor 2/hsf2 gene
	G5G8T7	hsf2
	190J12T7	AtHSF4, Heat Shock Factor 4
	125H21T7	AtHSF4, Heat Shock Factor 4
	201D9T7	HS21
	183O20T7	AtHSF21
	183D14T7	HSF-type DNA-bind domain
LHC-Like-Factors	129F10T7	Lil3, LHC protein
	F5E3T7	Lil3:1, LHC protein
	E7C4T7	Lil3:1, LHC protein
	E3H12T7	Lil3:1, LHC protein
ABRE-Binding Factors and Drought Related Factors	186P13T7	STZ, salt tolerant zinc finger protein
	202K22T7	DRE/CRT binding protein/drought high salinity responsive
	F2C8T7	ABRE-Binding Factor
MYC-type Factors	251I8T7	putative MYC
	134I5T7	putative MYC
Ethylene Response Element Binding Factors	121G24T7	AtERF 5
GA Response Factor	138E4T7	RGA1 gene, GRS protein (negative GA response)
Other transcription factors	161D9T7	RUSH-1 alpha isolog
	110H10T7	NF-kappa-B-like
	H7D3T7	helicase-like factor
Controls	221J11T7	HisH3, Histone H3 gene
	110J3T7	HisH2A, Histone H2A isolog
	187A16T7	Act8, ACT8 actin 8 gene
	168H2T7	Act2, ACT2 actin 2 gene
	pA	polyA sequence
	Desa	Human Desmin cDNA
	Desb	Human Desmin cDNA
	sus1	Sucrose synthase 1
	Neb1	Human Nebulin cDNA
	Neb2	Human Nebulin cDNA
	eFl	elongation factor 1
	pBS	plasmid
<i>A. thaliana</i> transporters	Atpt1	AtPT1 Phosphate transporter
	Atnrt1	Low Affinity Nitrate Transporter (CHL1)
	Atnrt2.1	High Affinity Nitrate transporter

The shoot:root fresh weight ratio of 14-day-old plants was lowest with 0.1 mM NO₃⁻ and highest with 10 mM NO₃⁻ grown plants when compared with 0.5 mM NO₃⁻ control plants (Fig. 1). The addition of 5 mM Asn to the nutrient medium did not change the shoot:root ratio whereas 5 mM Gln led to a 40% increase. Compared with the effect of 10 mM NO₃⁻, this increase, however, was smaller (40% vs. 100%) and corresponded to different plant responses: in the case of the 10 mM NO₃⁻ treatment, the root weight per plant was markedly less than with control plants, whereas the shoots of Gln-treated plants were slightly larger than those of control plants. The root architecture of plants grown on the different N sources compared with 0.5 mM NO₃⁻-grown plants was further analyzed using OPTIMAS software and the results are

shown in Figure 2. All the N treatments tended to cause a reduction in the length of the primary roots, but the most significant reduction was with Asn-supplemented plants. The length of the branching zone (i.e. the distance from the primary root base to the youngest lateral root) was reduced the most significantly by 10 mM NO₃⁻, but also by 0.1 mM NO₃⁻ and Asn, while Gln had no effect. Total lateral root length was most significantly inhibited by 10 mM NO₃⁻ while Asn-grown plants had the longest total lateral root length. Total root length was the longest in Asn-grown plants, and the least in the 10 mM NO₃⁻-grown plants, corresponding to the increase and decrease in total lateral root length, respectively. Plants grown on 10 mM NO₃⁻ had the fewest number of lateral roots. The results indicate that plants grown on 10 mM NO₃⁻ have the

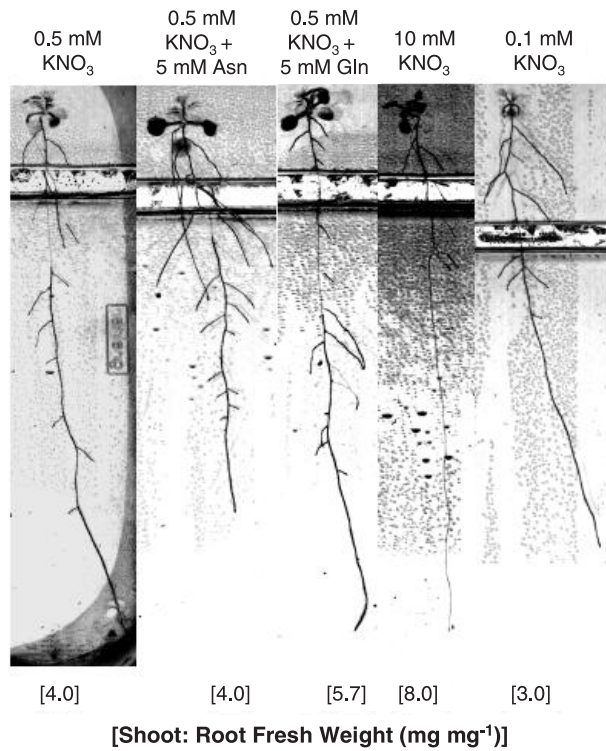


Figure 1. Representative plant images showing the influence of NO_3^- supply rate or amino acid supply on root architecture and shoot:root ratios of *A. thaliana* plants. Plants were grown on vertical Petri plates containing agar media segmented into two layers by a gap. The germination and the initial phases of growth thus occurred under identical conditions and every treatment (indicated above the plant images) was applied to the larger, bottom agar layer. All media contained identical amounts of macro- and micro-nutrients except for N which varied with the treatment; no carbohydrate was present. The experiments were repeated twice and more than 10 independent plants were analyzed in each experiment. The plants presented are typical of the branching patterns obtained. The values below the plant images correspond to the average shoot:root ratios (mg/mg fresh weight) of 5 plants.

shortest total length and lowest number of lateral roots of all the other treatments. In addition, plants grown on 0.5 mM NO_3^- supplemented with 5 mM Gln were the most similar to plants grown on 0.5 mM NO_3^- alone. Therefore, a potential screen to identify regulatory genes involved in the changes in root architecture in response to 10 mM NO_3^- , and not in response to changes in plant N status per se, can be developed by searching for genes expressed only in 10 mM NO_3^- and not Gln-grown plants, compared with 0.5 mM NO_3^- -grown plants.

In order to investigate the stage at which lateral root elongation was inhibited by 10 mM NO_3^- , a qualitative examination of the lateral root primordia of 10 mM NO_3^- -grown plants was performed and some representative images are shown in Figure 3. We found consistently that the lateral root primordia were initiated but unemerged from the primary root (Fig. 3 A, B and C). In contrast, very few lateral roots were observed to be emerged and inhibited at a later stage (Fig. 3 D and E).

A total of 126 putative transcription factor ESTs identified via BLAST searches of an EST database were arrayed on Nylon membranes as described in the Materials and methods. The macro-arrays were hybridized with ^{33}P -labeled cDNAs prepared from total RNA extracts from roots or shoots of 14-day-old plants grown on vertical agar plates containing either 0.5 mM or 10 mM KNO_3 or 0.5 mM KNO_3 plus 5 mM Gln with the same culture conditions used for the root architecture and morphology analysis. Each hybridization was performed with three membranes and the same set of three membranes were subsequently stripped and rehybridized with the cDNAs from each of the nitrogen treatments (i.e. 0.5 mM or 10 mM KNO_3 or 0.5 mM KNO_3 plus 5 mM Gln) and organs (i.e. roots and shoots). After the hybridizations, the arrays were scanned and spot intensities from the images were extracted and normalized as described in the Materials and methods. Images from a set of macro-arrays hybridized with either root or shoot cDNAs from 0.5 mM or 10 mM KNO_3 or 0.5 mM KNO_3 plus 5 mM Gln-grown plants are presented in Figure 4. The normalized averages of the spot intensities from

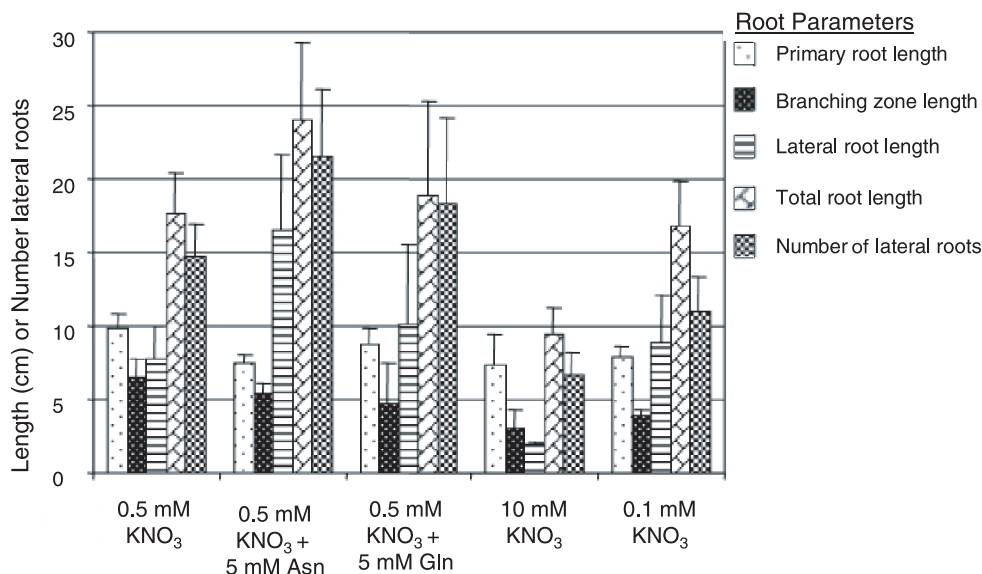


Figure 2. Effects of NO_3^- supply rate or amino acid supply on root architecture parameters of 14-day-old *A. thaliana* plants. Plants were grown for 14 days as in Figure 1 on media containing either 0.5 mM NO_3^- , 0.5 mM NO_3^- plus 5 mM Gln, 0.5 mM NO_3^- plus 5 mM Asn, 10 mM NO_3^- or 0.1 mM NO_3^- . The branching zone refers to the zone of the primary root from the hypocotyl down to the last emerged lateral root (i.e. the distance between the two lines represents the length from the tip to the youngest lateral root emerged). Plant images were scanned and analyzed as described in the Materials and methods. The results are the mean \pm se of five separate plants and the experiments were repeated twice.

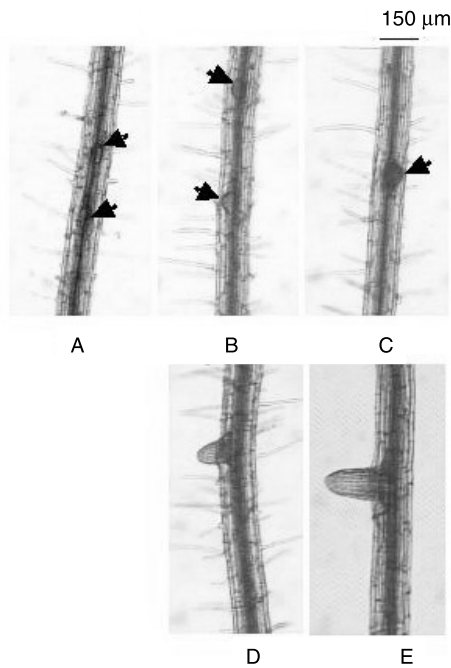


Figure 3. Effects of high NO_3^- on primordia initiation and development. The primary roots of 14-day-old *A. thaliana* plants grown as in Figure 1 were observed under a microscope. Arrows indicate unemerged lateral root primordia at stages typically observed with plants grown with 10 mM KNO_3 (A), (B), (C), and emerging lateral roots (D) and (E).

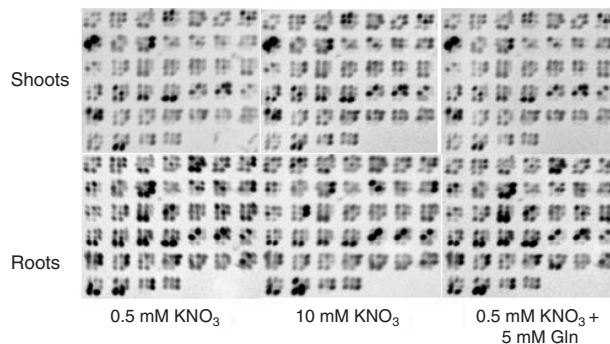


Figure 4. Transcription factor macro-array hybridizations. Representative images of transcription factor macro-arrays after hybridization with ^{33}P -labeled cDNA synthesized from total RNA isolated from roots (lower panels) and shoots (upper panels) of plants grown as in Figure 1.

hybridizations from two independent biological replicates (a total of 12 spot intensities per data point) are plotted in Figure 5. The root and shoot averages from 10 mM KNO_3 or Gln-grown plants (y axis) were plotted against the root and shoot averages of the 0.5 mM KNO_3 plants (x axis) and the r^2 coefficient from the resulting linear correlations were calculated. The roots of the 10 mM KNO_3 plants had the lowest r^2 value

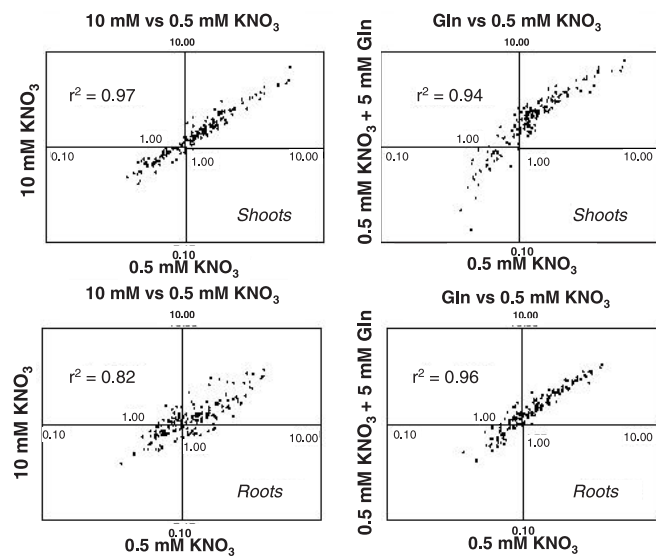


Figure 5. Graphical results of macro-array hybridizations. Graphical results of macro-array hybridizations from two independent biological replicates. Normalized average ratios of each N treatment (10 mM KNO_3 and 0.5 mM KNO_3 + 5 mM Glutamine) and organ were plotted against the normalized average ratios of the corresponding control tissue (0.5 mM KNO_3) on a logarithmic scale. Each point represents the average ratio of expression based on a total of 12 signal intensities for each treatment. The r^2 coefficient is based on the linear regression of each line.

($r^2 = 0.82$), indicating the highest variation in the signal intensities, and therefore the greatest changes in the transcript abundance occurred in the roots of plants grown under these conditions. The other treatments had similar r^2 values of 0.96 (Gln compared with 0.5 mM KNO_3 -grown roots), 0.94 (Gln compared with 0.5 mM KNO_3 -grown shoots) and 0.97 (10 mM KNO_3 compared with 0.5 mM KNO_3 -grown shoots), indicating less variation in transcript abundance in these samples. In general, the abundance of transcription factor transcripts changed the most in the roots of 10 mM KNO_3 -grown plants.

4. DISCUSSION

In this paper, we compared the effects of various N treatments on the root architecture of *A. thaliana* in order to develop a screen for regulatory genes involved in the response. All the N treatments examined modified the plant N status while they triggered different physiological and/or developmental responses. These treatments consisted of supplying NO_3^- at various concentrations with or without the addition of an amino acid. In the control treatment, N was supplied as 0.5 mM NO_3^- , a concentration which allowed optimal plant growth in our conditions and did not repress NO_3^- uptake or root development.

Consistent with previous reports in the literature [10, 15, 16], our results indicate that an increased NO_3^- supply favored shoot growth at the expense of root growth and led to a decrease in lateral root formation (Figs. 1 and 2, compare 0.1, 0.5 and 10 mM NO_3^- -grown plants). In contrast, Gln supply

stimulated the shoot growth rate but did not reduce the root growth rate, while Asn inhibited the primary root growth rate and stimulated lateral root growth. The fact that Gln and Asn had less effect on the shoot:root ratio compared with high NO_3^- (Fig. 1) is consistent with the findings that, in both tobacco [15] and *A. thaliana* [21], nitrate reductase-deficient plants are even more sensitive to the inhibitory effect of high NO_3^- . Analysis of the root branching pattern indicated that the production of root biomass differed from the 0.5 mM NO_3^- -grown plants in all the treatments except the Gln-treated plants. In summary, Asn-treated plants had more and longer lateral roots, 0.1 mM NO_3^- -grown plants had fewer lateral roots, and only the 10 mM NO_3^- -grown plants had both fewer, and a smaller total length of lateral roots. The high NO_3^- treatment resulted in the most significant reduction in the number and the total length of the lateral roots. In contrast, the root architecture of Gln-treated plants was the most similar to the 0.5 mM NO_3^- -grown plants. As reported elsewhere [16, 21], the inhibition of root growth by high NO_3^- is mainly due to a decreased number of lateral roots (Fig. 2). Consequently, the branching zone length was reduced in the 10 mM NO_3^- -grown plants. In contrast, none of the other treatments inhibited both lateral root development and the overall number of emerged lateral roots. Overall, high NO_3^- supply markedly decreased lateral root numbers and length, while Gln-treated plants were the most similar to the 0.5 mM NO_3^- -grown plants. In the roots, two sets of responses occur when the N resource level is changed; namely, modifications of NO_3^- transport capacity and of root architecture [17]. Both of these responses are complex and result from multiple regulatory pathways. Comparing the 10 mM NO_3^- and Gln-grown plants with 0.5 mM NO_3^- -grown plants, the effect on lateral root development is specific for the high NO_3^- treatment, which makes these culture conditions a good screen for isolating genes with expression that correlates to the root architecture response: while they have similar effects on NO_3^- transport [17], they have different effects on lateral root development.

Microscopic observation allowed us to examine the stage at which lateral root development was inhibited in the 10 mM NO_3^- -grown plants. We found that the high NO_3^- consistently arrested lateral root development at the stage just before emergence. According to the description by Malamy and Benfey [11, 12], this inhibition occurred between stages IV and VI of lateral root primordia development, at pre-emergence of the lateral root, prior to the activation of the meristem. Our results resemble those presented by Zhang et al. [21] for *A. thaliana* plants supplied with 50 mM NO_3^- , although in their case lateral root development was inhibited at a stage just after emergence (Fig. 3D).

To screen for regulatory genes involved in the N-related root plasticity response, we have initiated an approach using a macro-array which contains representatives of the major classes of transcriptional factors from *A. thaliana*. The N treatments discussed above (i.e. 0.5 mM NO_3^- , 10 mM NO_3^- and 0.5 mM NO_3^- supplemented with 5 mM Gln) were used as the sources of RNA for the cDNA synthesis and macro-array hybridizations. The highest variation in transcription factor transcript abundance was observed in the roots of the 10 mM NO_3^- plants when compared with the roots of Gln plants, or the shoots of Gln or 10 mM NO_3^- plants (Fig. 5). This varia-

tion correlates to the observed phenotypic response (e.g. the inhibition of lateral root emergence) of the roots of 10 mM NO_3^- plants and suggests a coordinated response that is complex and/or linked to multiple cellular processes. These results suggest the N culture conditions selected together with the macro-array approach may allow the identification of genes involved in the N-related root plasticity response and not general sensing pathways of the plant nitrogen status or some regulatory mechanism of NO_3^- uptake.

In summary, characterizing the plant root response to N supply, we showed that root morphology, and consequently the architecture of the root system, on one hand, and NO_3^- uptake capacity on the other hand, are under the control of distinct regulatory pathways. Changing the plant nitrogen status by different treatments allowed us to build a screen to potentially identify genes with expression that correlate with the inhibition of lateral root emergence but not the repression of NO_3^- transporters. Using this macro-array approach, we recently identified genes for a basic leucine zipper (bZIP) and a LIM transcription factor and confirmed via Northern analysis that their expression is preferentially observed in the roots and correlated to the root response to nitrate availability [18].

Acknowledgments: We gratefully acknowledge Jörg Hoheisel and Marcel Scheideler, Deutsches Krebsforschungszentrum, Heidelberg, Germany, for providing the EST library and the array-related protocols; and Rémi Houlgatte, Béatrice Loriod and Katrin Nguyen at TAGC (Technologies Avancées pour le Génome et la Clinique, Centre d'Immunologie de Marseille-Luminy, France) for the array spotting facilities and protocols. This project was funded by the EU Biotechnology program BIO4 CT97 2231.

REFERENCES

- [1] Burns I., Short and long-term effects of a change in the spatial distribution of nitrate in the root zone on N uptake, growth and root development of young lettuce plants, *Plant Cell Environ.* 14 (1991) 21–33.
- [2] Bertucci F., Bernard K., Loriod B., Chang Y.C., Granjeaud S., Birnbaum D., Nguyen C., Peck K., Jordan B.R., Sensitivity issues in DNA array-based expression measurements and performance of nylon microarrays for small samples, *Hum. Mol. Genet.* 8 (1999) 1715–1722.
- [3] Chapin F.S. III, Walter C.H.S., Clarkson D.T., Growth response of barley and tomato to nitrogen stress and its control by abscisic acid, water relations and photosynthesis, *Planta* 173 (1988) 352–366.
- [4] Clarkson D.T., Touraine B., Morphological responses of plants to nitrate-deprivation: a role for abscisic acid?, in: Roy J., Garnier E., (Eds.), *A Whole Plant Perspective on Carbon-Nitrogen Interactions* SPB Academic Publishing, The Hague, 1994, pp. 187–196.
- [5] Drew M.C., Comparison of the effects of a localized supply of phosphate, nitrate, ammonium and potassium on the growth of the seminal root system, and the shoot, in barley, *New Phytol.* 75 (1975) 479–490.
- [6] Drew M.C., Saker L.R., Nutrient supply and the growth of the seminal root system of barley. II. Localized, compensatory increases in lateral root growth and rates of nitrate uptake when nitrate supply is restricted to only part of the root system, *J. Exp. Bot.* 26 (1975) 79–90.
- [7] Ericsson T., Growth and shoot: root ratio of seedlings in relation to nutrient availability, *Plant and Soil* 168–169 (1995) 205–214.
- [8] Granato T.C., Raper C.D. Jr., Proliferation of maize (*Zea mays* L.) roots in response to localized supply of nitrate, *J. Exp. Bot.* 40 (1989) 263–275.

- [9] Hirose T., Kitajima K., Nitrogen uptake and plant growth. I. Effect of nitrogen removal on growth of *Polygonum cuspidatum*, *Ann. Bot.* 85 (1986) 479–486.
- [10] Lambers H., Cambridge M.L., Konings H., Pons T.L., Causes and Consequences of Variation in Growth Rate and Productivity of Higher Plants, SPB Academic Publishing bv, The Hague, The Netherlands, 1990, 363 p.
- [11] Malamy J.E., Benfey P.N., Down and out in Arabidopsis: the formation of lateral roots, *Trends Plant Sci.* 2 (1997) 390–396.
- [12] Malamy J.E., Benfey P.N., Organization and cell differentiation in lateral roots of *Arabidopsis thaliana*, *Development* 124 (1997) 33–44.
- [13] Raper C.D., Osmond D.L., Wann M., Weeks W.W., Interdependence of root and shoot activities in determining nitrogen uptake rate of roots, *Bot. Gaz.* 139 (1978) 289–294.
- [14] Robinson D., Linehan D.J., Caul S., What limits nitrate uptake from soil?, *Plant Cell Environ.* 14 (1991) 77–85.
- [15] Scheible W.R., Lauerer M., Schulze E.D., Caboche M., Stitt M., Accumulation of nitrate in the shoot acts as a signal to regulate shoot-root allocation in tobacco, *Plant J.* 11 (1997) 671–691.
- [16] Stitt M., Feil R., Lateral root frequency decreases when nitrate accumulates in tobacco transformants with low nitrate reductase activity: consequences for the regulation of biomass partitioning between shoots and root, *Plant and Soil* 215 (1999) 143–153.
- [17] Touraine B., Daniel-Vedele F., Forde B.G., Nitrate uptake and its regulation, in: Lea P.J., Morot-Gaudry J.-F. (Eds.), *Plant Nitrogen*, INRA-Editions and Springer-Verlag, Berlin-Heidelberg, 2001, pp. 1–36.
- [18] Tranbarger T.J., Al-Ghazi Y., Teyssendier de la Serve B., Muller B., Doumas P., Touraine B., Transcription factor genes with expression correlated to nitrate related root plasticity of *Arabidopsis thaliana*, *Plant Cell Environ.* 26 (2003) 459–469.
- [19] Walch-Liu P., Neumann G., Bangerth F., Engels C., Rapid effects of nitrogen form on leaf morphogenesis in tobacco, *J. Exp. Bot.* 51 (2000) 227–237.
- [20] Zhang H., Forde B.G., An Arabidopsis MADS box gene that controls nutrient-induced changes in root architecture, *Science* 279 (1998) 407–409.
- [21] Zhang H., Jennings A., Barlow P.W., Forde B.G., Dual pathways for regulation of root branching by nitrate, *Proc. Natl. Acad. Sci. USA* 96 (1999) 6529–6534.